

RPN36

PULSED ELECTRON BEAM STUDIES
AT 50,000 AMPERES AND 5 MeV

PIPB-9

by

Franklin C. Ford, William T. Link, and John Creedon

August 19, 1966

Physics International Company
2700 Merced Street
San Leandro, California 94577

CONTENTS

	<u>Page</u>
I. INTRODUCTION	1
II. THE PULSED POWER GENERATOR	2
III. ELECTRON BEAM PHENOMENOLOGY	6
A. Space Charge Effects in Vacuum	6
B. Gas Interactions	11
C. Image Forces	12
D. Magnetic Field Interactions	14
E. Beam Divergence and Angular Deviation	14
IV. CONVERSION TO OTHER RADIATIONS	15
References	16

LIST OF FIGURES

	<u>Page</u>
Figure 1. Block Diagram of Pulsed Power System	1
Figure 2. Typical Surge Generator and Coaxial Blumlein Line	4
Figure 3. Flash X-Ray Tube	5
Figure 4. Characteristics of Bremsstrahlung Produced by Megavolt Pulsed X-Ray System	7
Figure 5. Unneutralized Electron Beam	9
Figure 6. Beam and Equipotentials in Drift Chamber	10
Figure 7. Self-Photographs of the Electron Beam at Various Air Pressures	13
Figure 8. Image Charges and Currents	12
Figure 9. Self-Photograph of the Electron Beam in a Metallic Channel	14

MR CHAIRMAN - PROFESSOR HUBER

15 MIN

MEMBERS OF VULLEX

+ DISCUSSION

LADIES & GENTLEMEN.

COPIES OF MY PAPER MAY BE OBTAINED BY ASKING FOR THE CORRECT SESSION/AUTHOR CATEGORY AT THE DESK DOWN STAIRS

I. INTRODUCTION [SINCE MANY DO NOT HAVE COPIES OF THE PAPER

As the technology of pulsed power systems expands, new possibilities are created for the development of multi-megawatt electron accelerators. Recently developed pulsed power systems are capable of producing single-pulse electron beam currents of several hundred thousand amperes in the megavolt range, and a million amperes is a realistic possibility. The electron beam of these terrawatt pulsed power systems has been extracted through the anode region and is available for direct electron-beam interaction studies.

KNOW LITTLE ABOUT US, I'LL TRY TO STICK + STAY WITH TEXT.

Current research with the 40,000-ampere, 4-MeV external electron beam of the Physics International Company pulsed power system has led to a much wider understanding of the high-current-density beam and its behavior in vacuum and gases, as well as the nature of its interactions with dielectrics, conductors, and magnetic fields.

A description of the pulsed power system and many of the basic experiments performed with high-current external electron beams is presented as a means of disclosing the remarkable capabilities of the most recently developed pulsed power systems and their potential for industrial research applications.

- (§ + 8) BIO-MEDICAL RADIOGRAPHY
- CHEMICAL REACTIONS OF RADIOCHEMISTRY (CHEMICAL SYNTHESIS)
- ACTIVATION (BOTH NEUTRON INDUCED & γ INDUCED)
- RADIATION EFFECTS ON ELECTRONICS & OTHER MATERIALS (BOTH RATE FRAGMENTATION & DOSE DEPENDENT)
- IONIZATION
- RAPID ENERGY DEPOSITION APPLICATIONS, (VAPORIZATION, PRESSURE EFFECTS, SPALL,

$$\frac{4 \times 10^6 \times 4 \times 10^4}{10^{-2}} = 16 \times 10^{12} = 1.6 \times 10^{13} \text{ (watts/cm}^2\text{)}$$

II. THE PULSED POWER GENERATOR

The basic components of the Physics International Company high-voltage, high-current generator used in the external electron-beam experiments are shown in Figure 1.

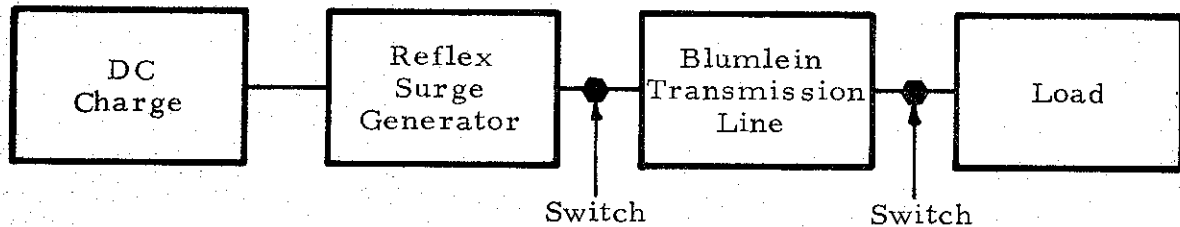


FIGURE 1. BLOCK DIAGRAM OF PULSED POWER SYSTEM

The general design philosophy followed minimizes the dc-charge levels and emphasizes the use of pulse-charge for the higher voltage levels. The major reason behind this philosophy is the desire to eliminate special corona and breakdown problems of high-voltage dc systems. The pulse charge system has resulted in a modular unit construction capable of being expanded as the need and technology advance.

The features of the particular high-voltage pulsed power system indicated in Figure 1 include a standard constant-current, high-voltage charging supply, a modular unit reflex surge generator similar to the conventional Marx surge voltage generator as the first-stage voltage multiplication system, and a resonance-charged coaxial Blumlein line serving as a high-voltage, low-impedance, pulse-forming, fixed-pulse-length, practical transmission line. The entire system is protected against corona discharge and voltage breakdown by the use of an oil dielectric covering all components except the load. Since the pulse duration of an electrical line, such as the coaxial Blumlein line, is given by two times the length of the line divided by the velocity of light in the dielectric medium of the line, the oil extends the pulse duration of a

given physical-length line over its vacuum value by a factor equal to the square root of the dielectric constant of the medium.

The operational features and characteristics of the high-voltage unit can best be described in terms of the following brief description of the operational cycle. The dc-charge unit, normally a standard 150-kV constant-current system, supplies voltage to the reflex surge generator. The design of the reflex surge generator involves parallel dc charge to a desired voltage V_0 of N modular capacitor units through resistive or inductive isolation circuits. Upon application of a suitable trigger, the capacitor modules of the reflex surge generator switch to a series configuration providing an output voltage of approximately NV . Figure 2 shows a typical surge generator and coaxial Blumlein line.

The charge of the reflex surge generator is transferred to the coaxial Blumlein line through an output switch and a resonance-charging inductor. The final maximum voltage on the Blumlein line for all practical cases of small circuit resistance is given by

$$V_f = \frac{2C_1}{C_1 + C_2} NV_0$$

The terms C_1 and C_2 are the surge generator and Blumlein line capacitance, respectively. The maximum final Blumlein line voltage is thus $2 NV_0$. The high-voltage Blumlein line is command-trigger-switched into the load, delivering $2 NV_0$ to a matched load, and the cycle is completed.

The Blumlein circuit, developed by the English radar expert Blumlein, is a practical high-voltage transmission line that permits full line-charging voltage to be applied to a matched load following command switching but completely isolates the load during the charging cycle. In essence, it is a two-stage voltage generator that feeds a conventional coaxial line attached to the load. The presence of the Blumlein line again permits operation at ^{the lowest} ~~the lowest possible~~ dc-charge and surge-generator charge for a given output voltage to a matched load. A 50-stage surge generator starting with an initial charge voltage of less than 150 kV can thus produce an

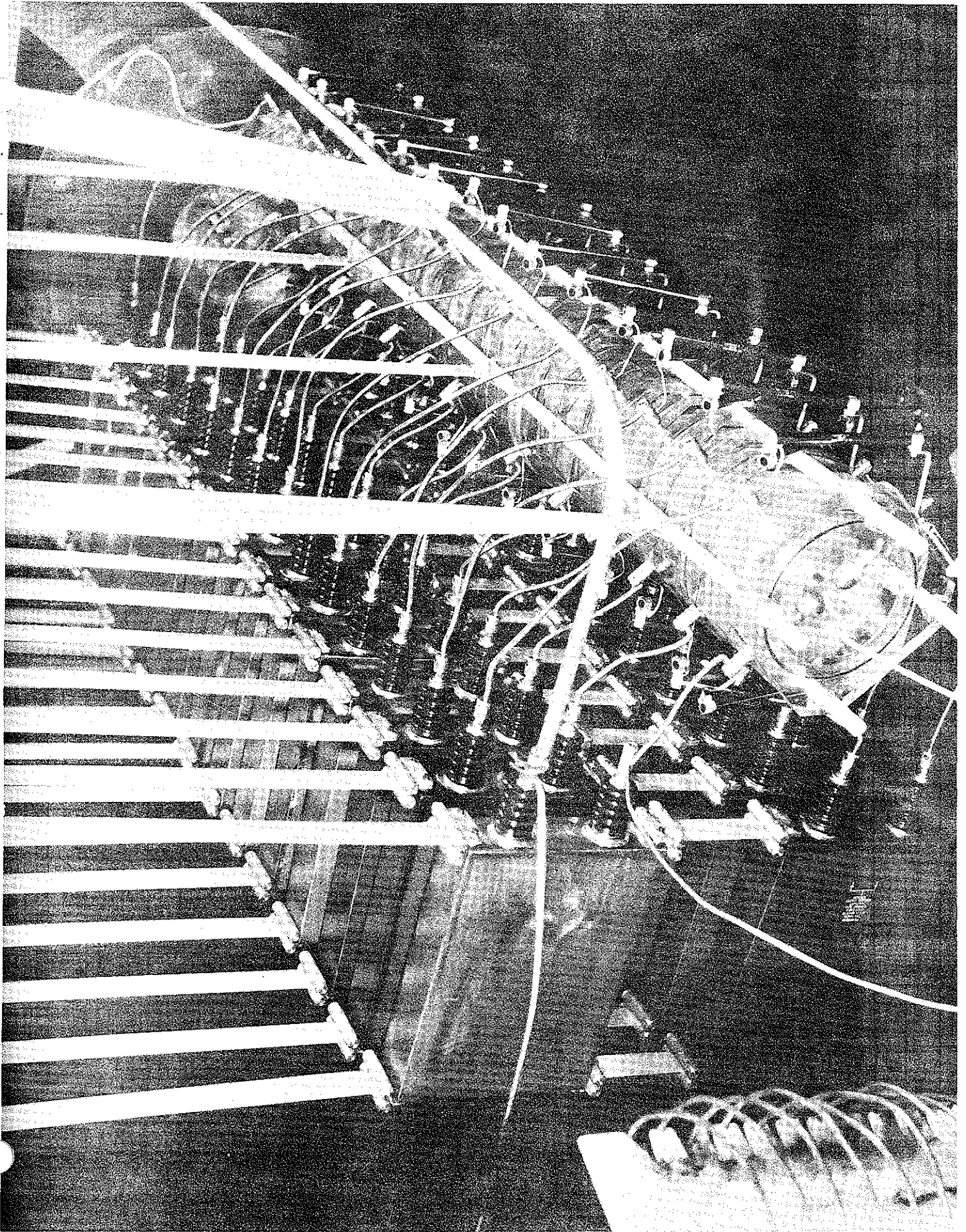


FIGURE 2. TYPICAL SURGE GENERATOR AND COAXIAL BLUMLEIN LINE

output voltage of 10 MeV across a matched load. A high-voltage generator of this type produces much higher voltages into appropriately selected mismatched loads. It is versatile enough so that it can be used as a power source for exploding wires, pulsed light sources, rapidly rising electromagnetic fields and currents for plasma heating, general laboratory high-voltage test systems, vacuum arc generators, and for producing intense electron beams in vacuum-gap systems by the field-emission process.

In this latter application, the vacuum-dielectric interface between the power source and the cathode-anode gap has been the subject of extensive investigations (Refs. 1, 2, 3). As a result of the early investigations, multimegavolt flash X-ray tubes were developed that produced intense bremsstrahlung radiation at levels of up to 10 R at a meter for pulse durations less than 100 nsec. The typical structures developed and used by J. C. Martin, Atomic Weapons Research Establishment, are shown in Figure 3.

These compact high-stress insulator structures exploit the principle of electrostatic sweeping of the insulator surface and utilize an end window-type anode structure. They can withstand more than five times the field

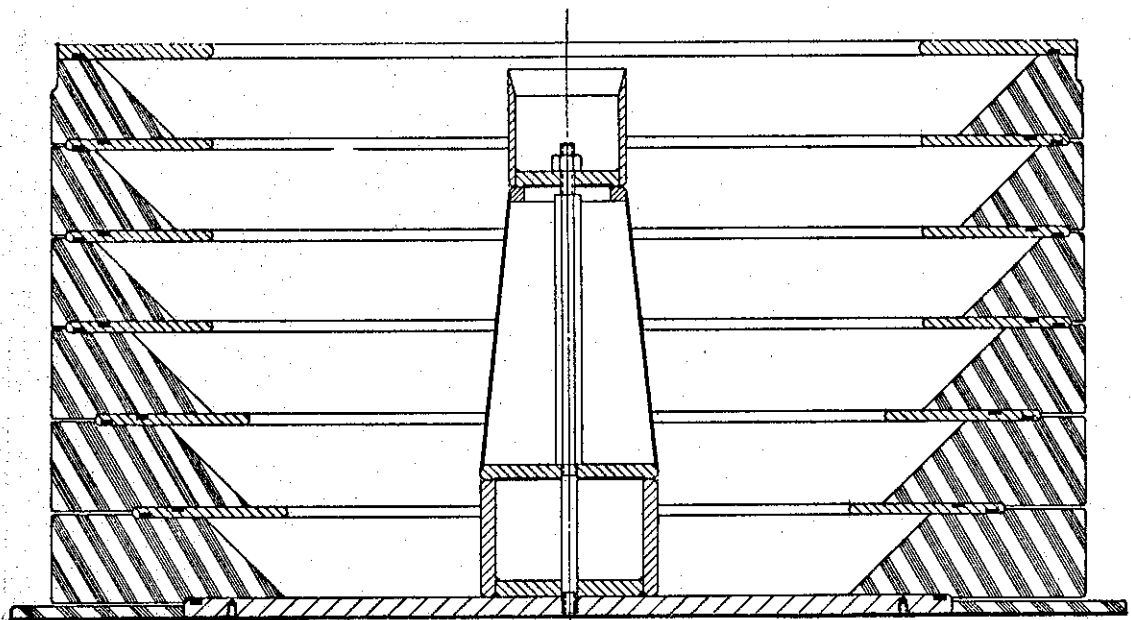


FIGURE 3. FLASH X-RAY TUBE

strength of a right cylindrical insulator for pulsed voltages. The impedance of such structures is generally in the range of 100 ohms. The results of the early investigations have been reviewed and extended to provide reliable, reproducible pulses at levels up to 200,000 V/cm along the vacuum-dielectric interface. The impedance level of the tube structure has been reduced to 25 ohms in these investigations.

Outputs of existing systems have reached levels of 100,000 amperes at 5 MeV, and a 400,000-ampere, 10-MeV system is being fabricated. Electron bombardment of the end window anode produces intense bremsstrahlung pulses (Ref. 4). The characteristic bremsstrahlung radiation produced by electron bombardment of the end window anode is shown in Figure 4.

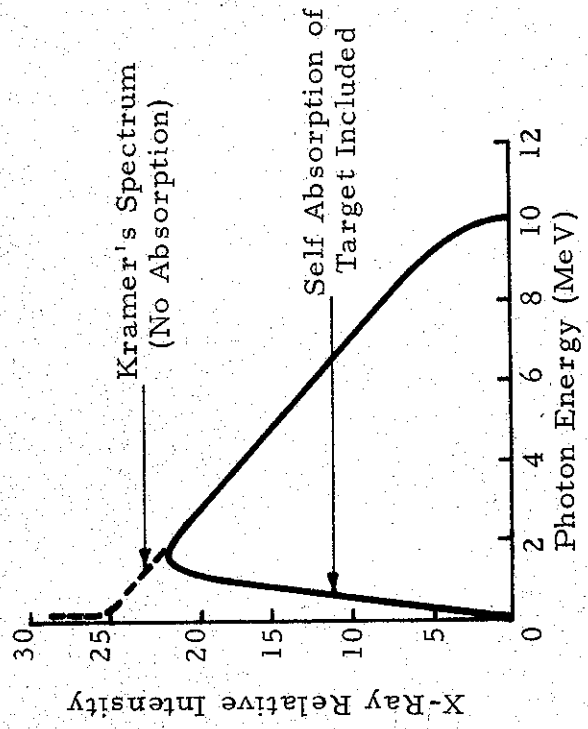
Research at Physics International has led to extraction of the electron beam through the anode structure of the pulsed X-ray tube. Investigations have been conducted on an analytical and experimental basis to determine the characteristics of the beam and its phenomenological behavior in vacuum and gases, and the nature of its interactions with dielectrics, conductors, and external magnetic fields.

III. ELECTRON BEAM PHENOMENOLOGY

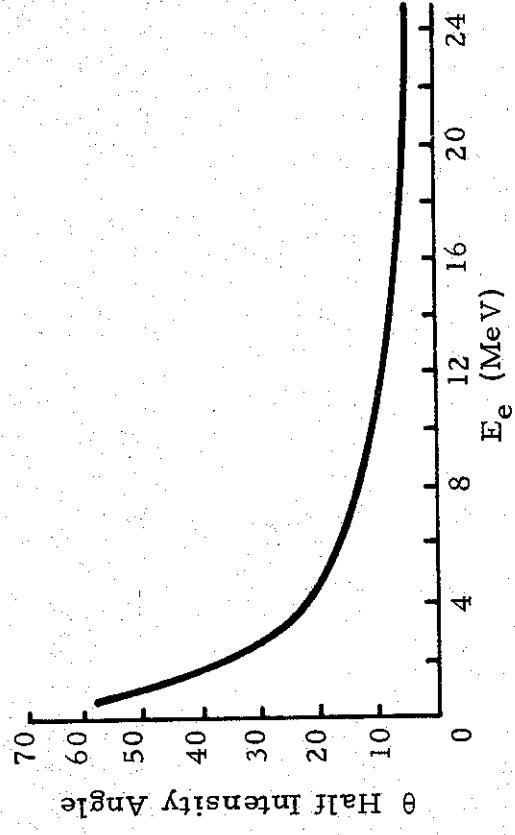
A. Space Charge Effects in Vacuum

1. Beam Spreading Due to Space Charge

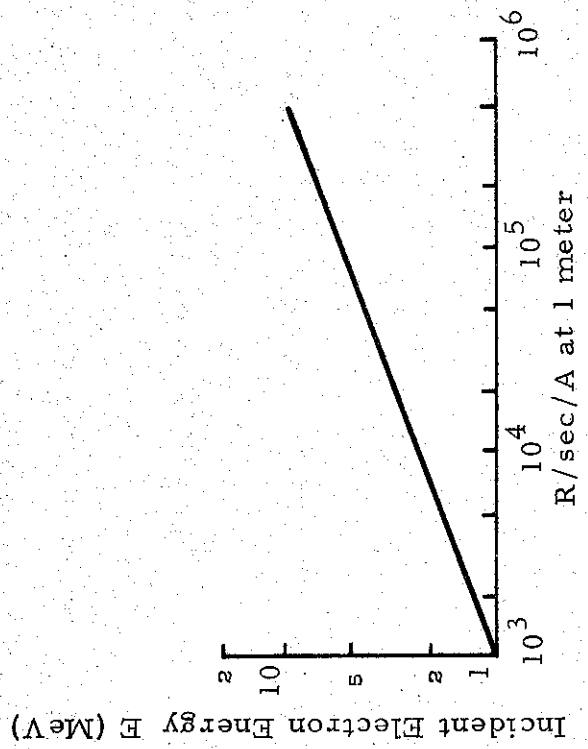
After the electron beam has passed through the foil anode into a region that is free of external fields (drift space), one is mainly interested in the spreading and loss of energy that occurs due to the self-field of the beam. Studies of the behavior of relativistic electron beams in vacuum regions have been conducted by many authors (Refs. 5, 6, 7). The following treatment is essentially that of Lawson (Ref. 7). The assumptions are: (1) steady state, (2) no longitudinal electrical field, (3) forces due to electric and magnetic fields are radial (i. e. the results are valid only for small angles of divergences), (4) beam initially parallel, (5) uniform current density throughout the beam.



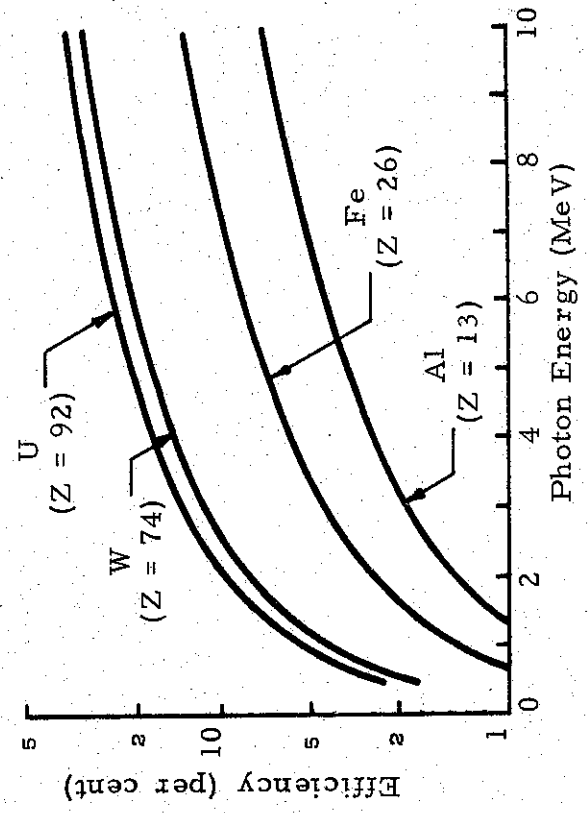
(a) Bremsstrahlung Spectrum for 10-MeV Electrons



(c) Angle of Half-Intensity as a Function of Initial Electron Intensity



(b) Forward X-Ray Yield for Tungsten (1 MeV < 10 MeV)



(d) X-Ray Production Efficiency for Various Target Materials

FIGURE 4. CHARACTERISTICS OF BREMSSTRAHLUNG PRODUCED BY MEGAVOLT PULSED X-RAY SYSTEM

For an electron beam in a region of hard vacuum, the radial electric field and the azimuthal magnetic fields are given (in Gaussian units) by

$$E = \frac{2Ne^2 r}{r_0^2} \quad B = \frac{2Ne\beta r}{r_0^2}$$

where E = radial electric field
 B = azimuthal magnetic field
 N = number of electrons per unit length
 e = electronic charge
 $\beta = v/c$

$v = \frac{dz}{dt}$ = electron velocity
 Z = axial distance in the drift region
 c = velocity of light
 r_0 = beam radius
 r = radius at which E and B are observed ($r \geq r_0$)

The electrons in the beam experience an outward force due to the electric field of the space charge and an inward force due to the magnetic field.

One can write down the
 The force on an electron at the edge of the beam ($r = r_0$) is:

$$\vec{F} = e \left(\vec{E} + \frac{\vec{v} \times \vec{B}}{c} \right) \quad (1)$$

$$F = \frac{2Ne^2}{r} (1 - \beta^2)$$

The differential equation of the motion for an electron at the edge of the beam is given by

AND OBTAIN A FIRST ORDER SOLUTION IN TERMS OF

$$\gamma m_0 \frac{d^2 r}{dt^2} = \frac{2Ne^2}{r} (1 - \beta^2)$$

where m_0 = electron rest mass
 $\gamma = (1 - \beta^2)^{-1/2}$
 t = time

Making the substitutions $\frac{d^2 r}{dt^2} = \beta^2 c^2 \frac{d^2 r}{dZ^2}$ and $v = \frac{Ne^2}{m_0 c^2}$

one gets $r \frac{d^2 r}{dZ^2} = \frac{2v}{\beta^2 \gamma} (1 - \beta^2) = K.$

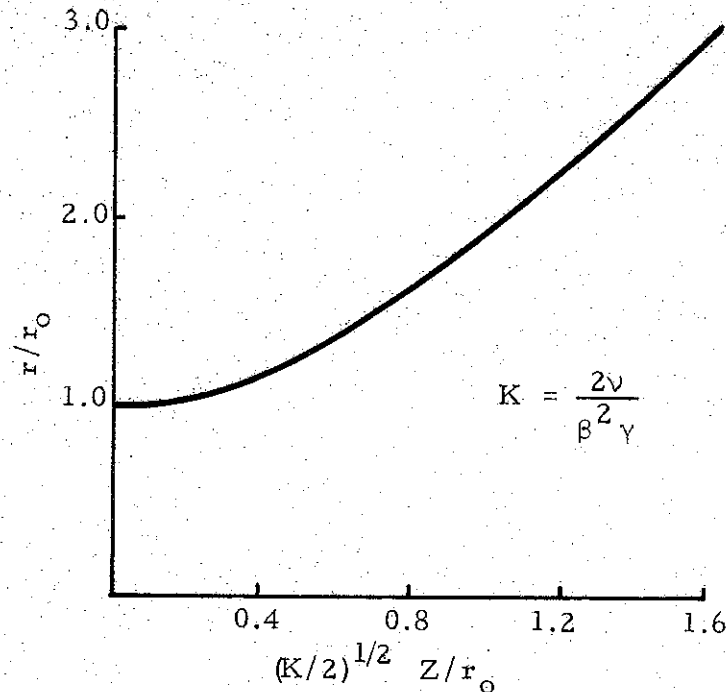
A DIMENSIONLESS

The quantity K is a dimensionless constant that is a generalization of the concept of perveance applicable to relativistic electron beams.

The solution of the differential equation is:

$$\frac{Z}{r_0} = \left(\frac{2}{K}\right)^{1/2} \int_0^{\ln \frac{r}{r_0}} e^{\mu/2} d\mu \quad (2)$$

where r_0 is the initial radius of the electron beam. This expression is plotted in Figure 5. SOLUTION



$$\gamma = \frac{1}{\sqrt{1-\beta^2}} \quad \beta = \frac{v}{c}$$

FIGURE 5. UNNEUTRALIZED ELECTRON BEAM (Initially Parallel)
 r = beam radius, Z = axial distance, r_0 = initial radius ($Z = 0$)

2. Longitudinal Electric Fields Due to Space Charge

The previous ~~treatment~~ ^{SOLUTION} neglected the effects of longitudinal electric fields due to space charge. An exact solution of this problem would be quite complex, but a useful approximation can be made for the conditions of steady state; no radial spread of the beam; beam in a cylindrical conducting drift chamber-- surface of the chamber an equipotential; and length of the chamber much greater than the diameter.

Figure 6 illustrates the arrangement of the beam and the equipotential surfaces inside the drift chamber. In the center of the drift chamber the

electric field is approximately radial ($Z_2 \gg r_2$), and one may use Gauss's law to obtain the electric field (mks units).

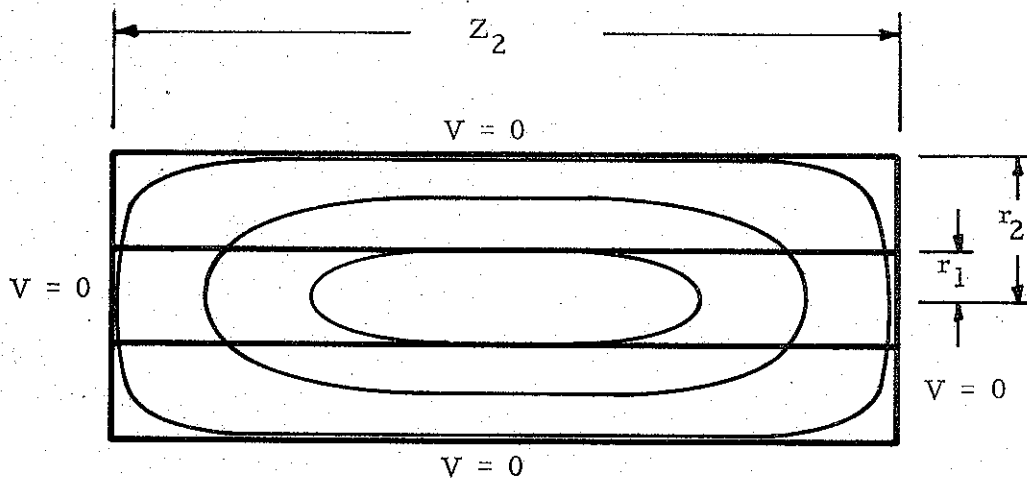


FIGURE 6. BEAM AND EQUIPOTENTIALS IN DRIFT CHAMBER

$$E = \frac{\rho r_1^2}{2r\epsilon_0} \quad r_1 \leq r \leq r_2$$

$$E = \frac{\rho r}{2\epsilon_0} \quad 0 \leq r \leq r_1$$

where ρ = charge density
 r = radial position
 r_1 = beam radius

r_2 = chamber radius
 $\epsilon_0 = 8.85 \times 10^{-12}$

If the potential of the drift chamber is taken to be zero, the potential inside the chamber (for $Z = \frac{Z_2}{2}$) is given by

$$V = \frac{60I}{\beta} \left[\ln \frac{r_2}{r} \right] \quad r_1 \leq r \leq r_2$$

$$V = \frac{60I}{\beta} \left[\ln \frac{r_2}{r_1} + \frac{1}{2} - \frac{1}{2} \frac{r^2}{r_1^2} \right] \quad 0 \leq r \leq r_1$$

where $I = \rho \beta c [\pi r_1^2] =$ beam current

I and V are, of course, negative for an electron beam.

2269

NECESSITY OF THE NEED OF A MORE EXACT SOLUTION

As an example, consider a 40,000-amp, 4-MeV beam in a drift tube. The potential on axis ($r = 0$) at the center of the tube is $V = -2.86 \times 10^6$ volts. From Figure 5, this beam would travel 20 cm before expanding one beam radius.

The approximations involved in Expressions 2 and 3 are obviously not valid for a 40,000-amp, 4-MeV beam (i. e., the reduction in kinetic energy due to longitudinal electric field would certainly result in large radial spreading ^{of the beam}), but one can use these expressions to calculate the approximate current levels that can be transported in a hard vacuum.

In order to transport the high-current-level electron beams available from Physics International pulsed power systems, it is necessary to fill the drift chamber with gas so that the ions created during beam transmission will partially neutralize the effects of the electron space charge.

B. Gas Interactions

If the electron beam experimental chamber is filled with a low-pressure gas, the self-forces in the beam may be strongly modified. The high-energy electrons ionize the gas, and the released electrons are then repelled by the large radial electric fields. The remaining positive ions tend to electrically neutralize the electron beam.

The rapid rise of magnetic field when the electron beam passes through the experimental chamber may induce large back currents that reduce the magnetic field of the primary electron beam.

If the electric field is ^{reduced} by the factor f_e and the magnetic field by the factor f_m , ~~Equation (1) becomes~~ *the beam can be controlled over a wide variety of density levels*

$$F = \frac{2Ne^2}{r_0} [1 - f_e - \beta^2(1 - f_m)] \quad (4)$$

For a wide range of gas pressures f_e is nearly unity, and the force experienced by high-energy electrons is due primarily to the magnetic effect

and becomes negative, or directed toward the beam axis. This is the condition for a self-pinch of the beam.

At air pressures from 0.01 Torr to 1 Torr, the beam is observed to be pinched, as is indicated in Figure 7b. Figures 7b, 7c, and 7d are examples of self-photographs of the recombination light from ions left in the wake of the electron beam.

As the air pressure rises above 1 Torr, the induced conductivity of the air increases, beam-induced back currents become large, and the factor f_m approaches unity. In this case the beam is both electrically and magnetically neutralized, and beam self-forces are greatly reduced. The beam drifts through the experimental chamber expanding with its own initial angle of divergence, as illustrated in Figure 7c. If the air pressure is raised further, the back currents decrease, and the beam again pinches, Figure 7d.

C. Image Forces

The existence of large beam self-forces suggests the possibility of large forces resulting from image charges and image currents in metallic surfaces. The electric charge in the beam induces opposite image charges in a metallic surface, while the time-varying magnetic fields of the beam induce eddy currents in a metallic surface that are equivalent to a single, oppositely directed image current. This is illustrated in Figure 8.

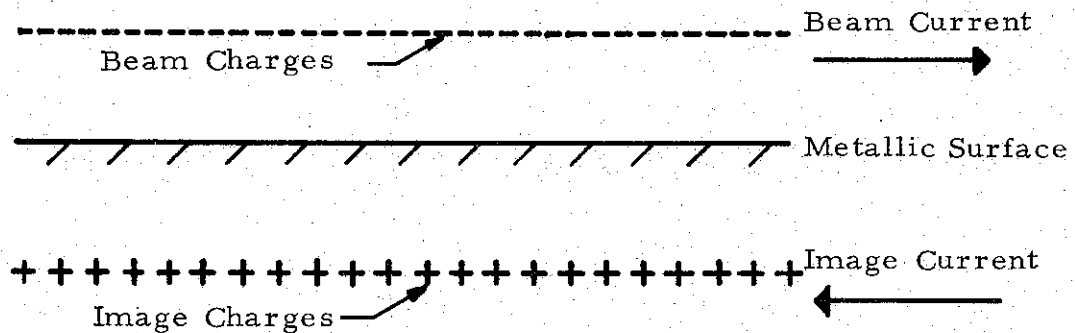
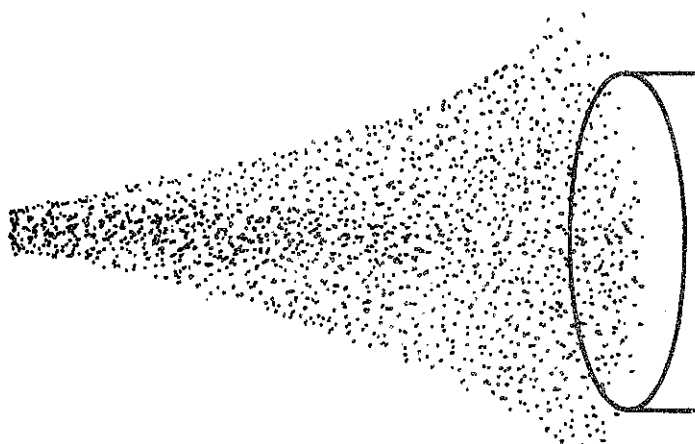


FIGURE 8. IMAGE CHARGES AND CURRENTS

Beam Direction

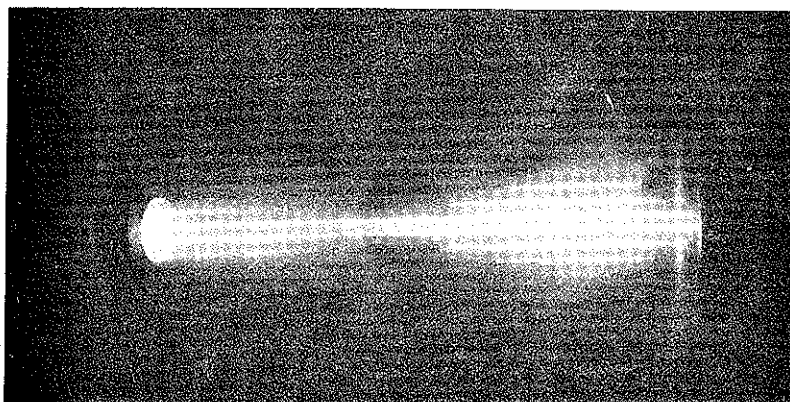


(a)

Pressure = 0

$f_e = f_m = 0$

F is large and positive



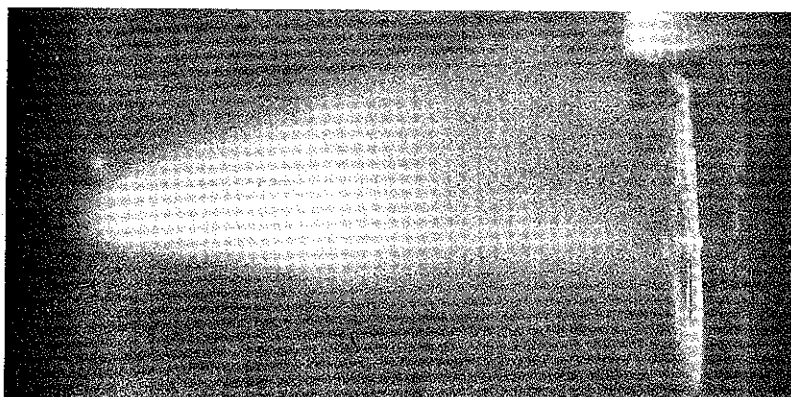
(b)

Pressure = 0.1 Torr

$f_e \approx 1$

f_m small

F is large and negative



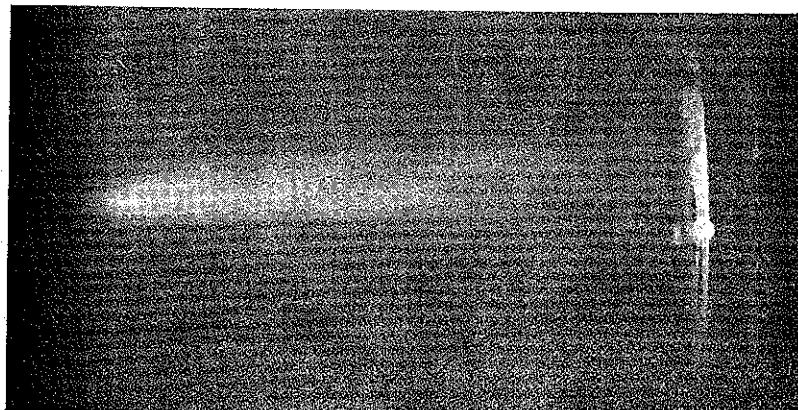
(c)

Pressure = 5 Torr

$f_e \approx 1$

$f_m \approx 1$

F is small



(d)

Pressure = 20 Torr

$f_e \approx 1$

$f_m < 1$

F is negative

FIGURE 7. SELF-PHOTOGRAPHS OF THE ELECTRON BEAM AT VARIOUS AIR PRESSURES

The force between charge and image charge is attractive, and the force between current and image current is repulsive. If electric neutralization is nearly complete ($f_e \sim 1$ in Eq. 4), the repulsive force predominates. Figure 9 is a self-photograph of an actual 40,000-amp, 4-MeV electron beam that has been fired into a metallic channel. The beam reflects from surface to surface in the channel much as light would reflect in a light guide. In this case the channel was too sharply curved to allow the electron beam to completely follow it.

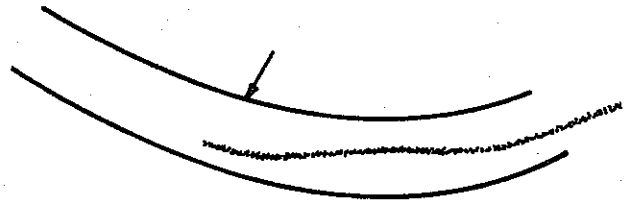
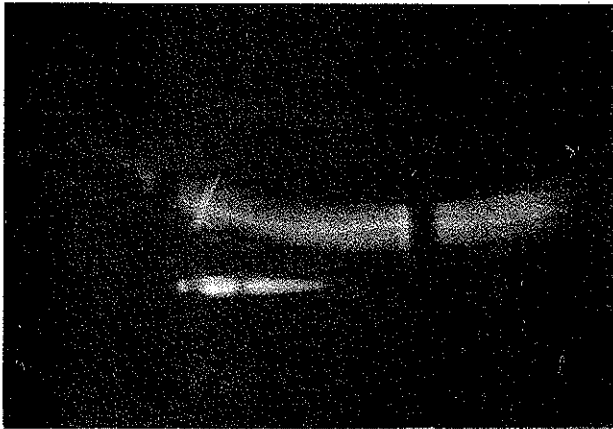


FIGURE 9. SELF-PHOTOGRAPH OF THE ELECTRON BEAM IN A METALLIC CHANNEL

D. Magnetic Field Interactions

The electron beam can and has been bent by a magnetic field (~ 2000 gauss) even when fully pinched. The internal self-forces of the beam make impossible the measurement of momentum distribution in a moderate magnetic field for the total beam. A portion of the beam sufficiently small to nearly eliminate the self-forces can, however, be magnetically analyzed in the usual way.

E. Beam Divergence and Angular Deviation

In twenty consecutive test shots at a pressure of 2.0 Torr the rms angular deviation of the electron beam from the experimental chamber axis was 3 deg with a half angle of 0.1 radian.

In a recent series of 40 test shots, the intensity per unit area was varied from 10 cal/cm² to 120 cal/cm² by changing the target-to-anode distance for each test. The predicted and measured values of intensity were in agreement to within 8 per cent.

IV. CONVERSION TO OTHER RADIATIONS

The electron beam can be converted to X rays by the bremsstrahlung process. It is also possible to produce a very-short-duration, high-intensity neutron pulse by the photo-neutron process. Beryllium, with a 1.67-MeV threshold, is the best target material for beam energies below 10 MeV.

Uranium, ^{is} the best target material for energies greater than 10 MeV, since it has a very large photo-neutron production cross section at higher energies. (ENERGY BACK SCATTERING)

(CONT) At electron-beam energies above 15 MeV, ion beams produced by counterstreaming positive ions become possible. At 20 MeV, for example, it is possible to have a proton beam current equal to 15 per cent of the electron beam current. For these very high pulsed power systems, the ion beam current could exceed a hundred thousand amperes.

FOR THOSE WHO WOULD LIKE TO
ASK ADDITIONAL QUESTIONS, I WILL
BE IN THE DEPT OF COMMERCE AREA
TOMORROW (AND IF
{ AT APPROXIMATELY 10⁰⁰ }
\$ 12⁰⁰ }